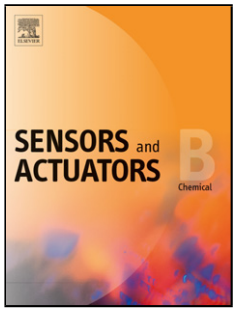

Title: Self-heating effects in large arrangements of randomly oriented carbon nanofibers: application to gas sensors

Author: O. Monereo J.D. Prades A. Cirera

PII: S0925-4005(15)00122-7
DOI: http://dx.doi.org/doi:10.1016/j.snb.2015.01.095
Reference: SNB 18022

To appear in: *Sensors and Actuators B*

Received date: 9-12-2014
Revised date: 9-1-2015
Accepted date: 24-1-2015

Please cite this article as: O. Monereo, J.D. Prades, Self-heating effects in large arrangements of randomly oriented carbon nanofibers: application to gas sensors, *Sensors and Actuators B: Chemical* (2015), http://dx.doi.org/10.1016/j.snb.2015.01.095

Self-heating effects in large arrangements of randomly oriented carbon nanofibers: application to gas sensors

O. Monereo*, J. D. Prades and A. Cirera
MIND-IN^{2}UB, Department of Electronics, University of Barcelona, C/ Martí i Franquès 1, E-08028 Barcelona, Spain

*Corresponding author e-mail: omonereo@el.ub.edu

Other authors e-mails: J.D. Prades (dprades@el.ub.edu), A.Cirera (acirera@el.ub.edu.)

Abstract. Herein, we prove that self-heating effects occur in sensor films made of randomly oriented nanoparticles (electro-sprayed, drop-casted and paint-brushed films of carbon nanofibers). A 2-point calibration method, reliable enough to overcome the lack of reproducibility of low cost fabrication methods, is also proposed. Self-heating operation makes possible reaching temperatures up to 250°C with power consumptions in the range of tens of mW. For certain low-temperature applications (<100°C) typical power consumptions are as low as tens of μW. The method is suitable to modulate the response towards gases, such as humidity, NH_3 or NO_2. This approach overcomes the complex fabrication requirements of previous self-heating investigations and opens the door to use this effect in cost-effective devices.

Keywords: self-heating**,** self-heating calibration**,** conductometric gas sensor**,** carbon nanofibers**,** humidity sensor.

Highlights:

- Self-heating effects in large arrays of randomly deposited carbon nanofibers are shown.
- Self-heating reduces power consumption from mW to μW.
- Self-heating in randomly deposited carbon nanofibers self-heating devices can be calibrated using a fast 2-point procedure.
- Humidity sensing is proven to be equivalent in external heater and self-heating operation, without changing the transduction sensing mechanism.
- NH_3 and NO_2 gas response modulation by self-heating is also shown.

1. Introduction

Conductometric gas sensors usually operate at high temperatures, typically from 100°C to 500°C [1], in order to optimize the sensor signal by tuning the chemical processes occurring at the surface of the active material. To that end, sensors are equipped with external heaters, which are the most energetically demanding component of the device. Commercial solid state gas sensors based in metal oxides typically require from 200mW to 1W to reach the operating

temperatures [2]. Most attempts to lower these power needs focus on: (1) Fabricating more efficient heating systems. (2) Using alternative sources of energy, such as ultraviolet light. (3) Modifying the active material to lower the temperature requirements.

The first approach focusses in lowering the heat losses, e.g. with micro-machined heaters mounted on thermally insulated membranes [2–4]. In the second case, an efficient light source (such as a LED) is integrated in the sensor device reaching power needs comparable to those of conventionally heated sensors [5–8]. In the third case, sensor active layer functionalization [9,10], material decoration [11,12] and the use of hybrid materials [11,13,14] are traditional strategies to enhance and modify the active film properties, and hence the gas-surface interaction mechanism. In one way or another, state of the art gas sensors still require more than 10-100mW (research devices) to maintain the elevated temperatures for good sensing performance, which limits their use in mobile distributed systems [15].

A more recent approach to solve this issue is harnessing the Joule dissipation that occurs in the sensor material itself. This so-called self-heating effect has been already studied in nanosized gas sensor devices [16–20], achieving very low power figures. Specifically, self-heating was first proven in one single SnO_2 nanowire, obtaining reliable devices operated with less than 10μW [18–22]. To the best of our knowledge, self-heating has further been studied in sensor devices with highly ordered nanostructures, such as suspended nanowires [15,19,20], or catalytically activated materials [17]. All these studies involved complex fabrication steps and laboratory fabrication methods hardly transferable to a higher production scale, hampering the widespread application of this promising approach. Here, we provide evidences that self-heating-modulated response to gases also occurs in randomly ordered nanomaterials deposited by simple and scalable methods such as electro-spraying, drop-casting and paint-brushing; achieving similar power savings than those observed in highly ordered nanostructures.

In the last few years, carbon nanomaterials have gained uprising interest as their electrical, optical and mechanical properties make them good candidates for a new generation of low-cost devices [23–26]. Carbon based structures can be obtained with many diverse techniques; e.g. chemical vapor deposition [27], arc discharge [28], pyrolysis [29], chemical [30] and thermal reduction [31], offering different materials qualities and scalability costs [32–34]. The gas sensing properties of carbon materials have been widely demonstrated [35–41]. In many carbon nanomaterials, sensing at room temperature or temperatures well below 100ºC is possible [24,35]. Some authors have proposed the use of pulses at moderate temperature just to "clean" the gas adsorbate from the surface [42]. Therefore the interest of heating in carbon materials is well different than in the case of metal oxide based gas sensor. In any case, the possibility to avoid the heater in the sensor substrate will significantly decrease the price of the device.

Self-heating effects have also been proven in individual carbon nanotubes operated with a few μW [15,43]. In this work, we used carbon nanofibers [44] (from now on CNFs), a carbon allotrope offering characteristics and sensing capabilities [41,45] comparable to carbon nanotubes and graphene [46] at a much lower production cost.

In this work, we show that the probing voltage (or current) used to interrogate the electrical resistance of a film of randomly distributed CNFs can be used to achieve gas responses similar to those obtained with an external heating element (i.e. self-heating). We also demonstrate that a simple 2-point calibration procedure is enough to determine the equivalent operation temperature. All this simplifies the use of self-heating dramatically, both in terms of fabrication requirements and operation procedures.

2. Materials and methods

2.1. Sensor fabrication

Interdigitated platinum electrodes (IDE) over a ceramic substrate with an integrated heater and a thermoresistance, fabricated by Francisco Albero S.A.U. [47], were used. The thermoresistance embedded in these devices was used for temperature calibration. Commercially available CNFs were synthesized by Grupo Antolín S.A. by means of CVD floating catalyst technique. The fibers presented diameters ranging from 30 to 80 nm and lengths up to 75μm, further details can be found elsewhere [48]. CNFs were dispersed in 2-propanol with a concentration of 1mg/ml, the resulting dispersion was stable for several days. Then, the CNFs' dispersion was electro-sprayed over the IDE (figure 1(a)-(c)), a voltage about 13kV was applied between an ejection syringe and a target electrode at a distance of 15 cm with deposition times ranging from 5 to 20 minutes. Other simple deposition techniques were also used for comparison, such as drop-casting and paint-brushing the same dispersion, obtaining equivalent functional properties (i.e. self-heating, calibration and response to gases). Electrical resistance was monitored during the deposition process with a digital multimeter Agilent 34401A to assess the continuity of the film. More than 20 different devices presenting resistance values ranging from hundreds of ohms to megaohms were studied in this work. Through this paper, error bars in figures correspond to the standard deviation of at least 5 measurements in equivalent conditions,

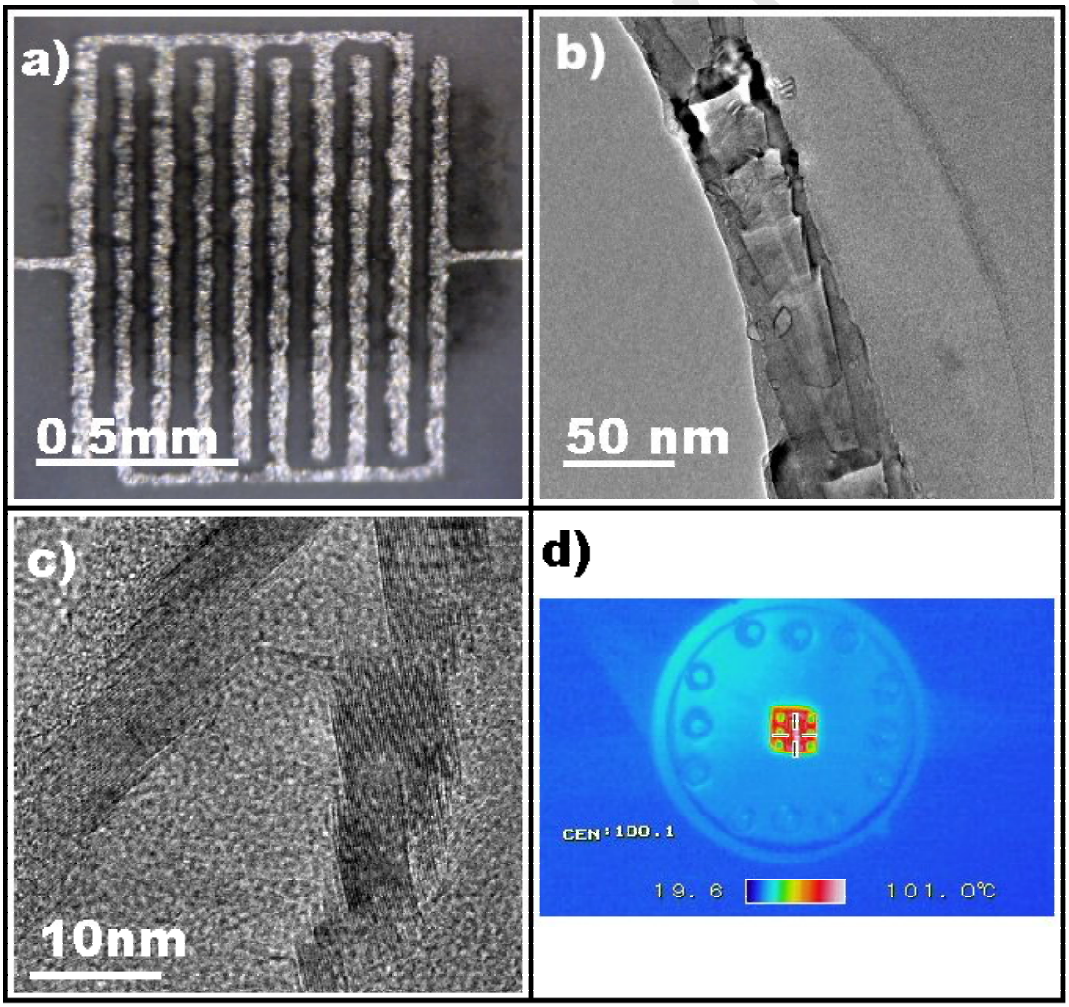

Figure 1. (a) Optical image of an electro-sprayed CNFs film over an IDE. (b) Transmission electron microscopy (TEM) image and (c) high resolution TEM image of a single CNF showing a fishbone–like structure of graphene platelets. (d) Termographic image of a CNF sensor with

an applied probing voltage of 5V to the CNFs film (CEN value correspond to the temperature in the central image point in ºC).

2.2. Gas sensing experiments

Self-heated sensors were calibrated in atmospheres of N_2 and synthetic air (SA, 21% in O_2 and 79% in N_2) as described below. Gas sensing experiments were conducted in a customized chamber of 15ml in volume, the gas flow was maintained at 200ml/min during all the experiments. Reference gaseous atmospheres were provided by several independent mass flows controllers blending N_2, SA, NH_3 (100ppm in SA) and NO_2 (10ppm in SA). Humid air was obtained by bubbling dry SA into deionized water. The gas sensing response was calculated according to the following definition: $\text{Response}(\%) = 100 \cdot (R - R_o)/R_o$, where R is the steady sensor resistance signal reached in each experiment and R_o is the baseline value of sensor resistance. Electrical measurements during gas test experiments were performed with a Keithley 2401 source-meter unit.

2.3. Temperature calibration

The deposition method offered no control on the microscopic arrangement of the CNFs over the IDE. Thus, a calibration step was necessary before operating them in self-heating mode. First, a temperature vs. resistance curve was obtained by means of the calibrated heater inside the ceramic substrate. Then, the resistance vs. the probing voltage applied to the CNFs film in self-heating operation was measured. Finally, combining the electrical resistance values of both curves; the calibration curve of temperature vs. probing voltage applied to the CNFs film was calculated. Alternative direct calibration procedures, such as thermography imaging, were also attempted and discarded: self-heating was qualitatively observed but the quantitative temperature estimations were found unreliable.

3. Results & Discussion

3.1. Self-heating in N_2 and SA atmosphere

Self-heated CNFs sensors were first tested in inert N_2 atmosphere. Figure 2(a) shows the sensor resistance during a calibration sequence. First, the heater temperature was increased in 5°C steps from 25°C to 110°C producing a sequential and reversible decrease in the CNFs resistance, which reveals their semiconductor character (see Figure 2(b)). Then, a similar resistance evolution was observed when increasing the probing voltage applied to the CNFs film in 0.5V steps from 1V to 10V. This result provides a first evidence of the self-heating effect occurring in the CNFs film. Figure 2(c) shows a calibration curve for that effect, obtained by correlating the resistance values of both measurements. The same experiment was repeated in SA atmosphere finding an equivalent behavior, with sensor resistance values shifted downwards due to a partial adsorption of oxygen molecules on the CNFs surface [49]. Additional direct evidences of the self-heating occurring in the film were obtained in thermographic images (see Figure 1(d)). However, this technique was not suitable for practical calibration purposes, as self-heating driven temperature varies widely across the film, making complex the assignment of a meaningful average temperature.

In all the experiments, a linear dependence of the temperature against the applied voltage was found, opening the door to define the simple calibration procedure proposed below. For small

temperature variations, the temperature dependence of the CNFs film resistance (so-called R in the previous section) can be regarded linear,

$$R = R_o\left[1-\alpha_{CNFs}\cdot\Delta T\right] \quad (1)$$

where R_o is the resistance of the CNFs at a reference temperature (in our case room temperature, 25°C), α_{CNFs} is the linear coefficient of dependence of resistance with temperature and ΔT is the temperature variation from reference conditions. In these conditions, the relationship between the dissipated electrical power and the temperature reached is:

$$P = \frac{V^2}{R} = \frac{V^2}{R_o\left[1-\alpha\cdot\Delta T\right]}, \quad (2)$$

which fits well the experimental observation (see Figure 2(d)).

The main advantage of the self-heating approach shows up when comparing the power needed to reach equivalent temperatures with both methods: for temperatures from 25°C to 250°C, power consumption in self-heating is reduced from 4 to 2 orders of magnitude with respect to the heater. In absolute values, our simplified approach to self-heating mode requires always less than 10mW, which is comparable to the needs of advanced micro-heaters [50].

Concerning the thermal response dynamics, thermal stabilization times were 7.2 ± 0.2 seconds in average for the temperature range under study.

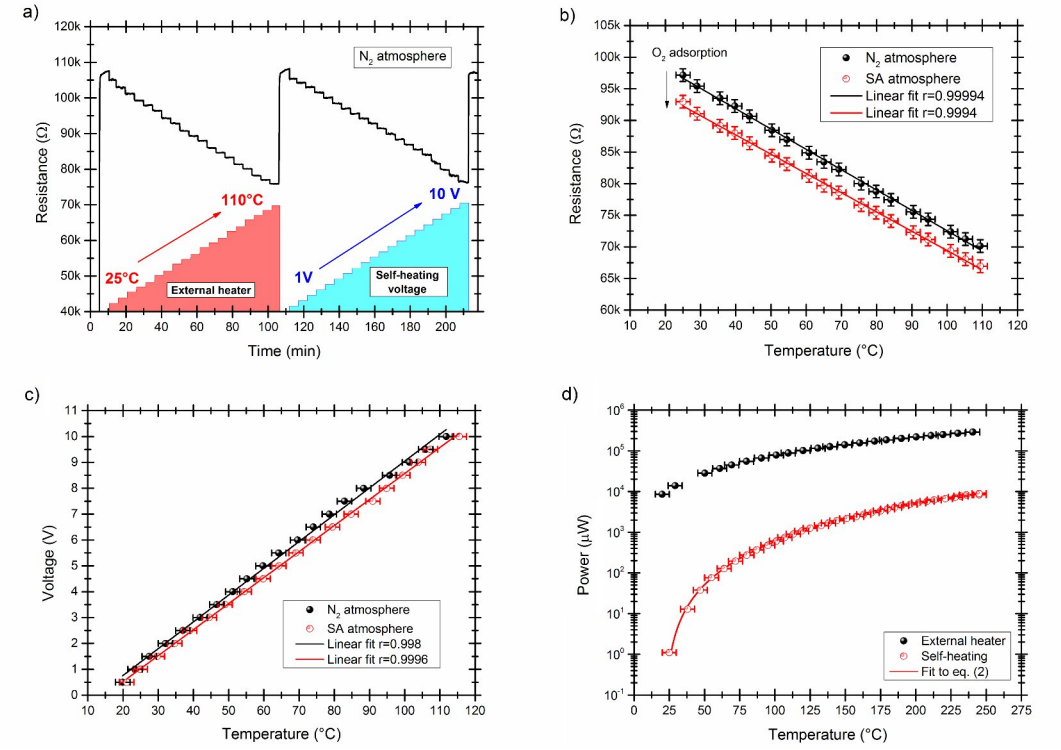

Figure 2. (a) Comparison of the resistance changes caused by temperature variations driven by an external heater and by the self-heating effect. (b) Sensor resistance vs. temperature curve obtained with an external heater (in N_2 and SA). (c) Calibration curves (voltage vs. temperature)

obtained correlating the value of CNFs resistance with the voltage applied to the film. (d) Comparison of the power needs of an external heater and the self-heating effect: the later reduces consumption more than two orders of magnitude. Datapoints were fitted to eq. (2), leading to $R_o = 9060.9 \pm 0.2\ \Omega$ and $\alpha = (9.23 \pm 0.01) \cdot 10^{-4}\ \Omega/K$, ($r = 0.9995$).

3.2. Endurance

3.2.1. Initial thermal stabilization

The deposition method leaves solvent residues in the as-deposited material that cause resistance drifts until solvents are fully removed. A good practice to overcome this issue is heating the material to reduce the evaporation time of the residues for full signal stabilization [41]. We observed that self-heating can also be used for that purpose. The as-deposited sensors were heated up and cooled down several times controlling the power applied to the film in self-heating operation. After the first warm up sequence, the sensors always showed fully reversible and repeatable resistance values (see Figure 3), even in long-term operation, as discussed next.

3.2.2. Stability, reversibility, repeatability

Sensors stability under self-heating conditions was also verified for several hours, alternating two voltages values (0.1V and 5.0V) applied to the CNFs film (inset in Figure 3). The sensor temperature oscillated between 25°C and 65°C showing no degeneration or any other significant change in resistance. Temperature was fully reversible and stability at each step was better than ±2°C. From a long term perspective, these features were again tested for repeatability showing similar results after numerous weeks since fabrication.

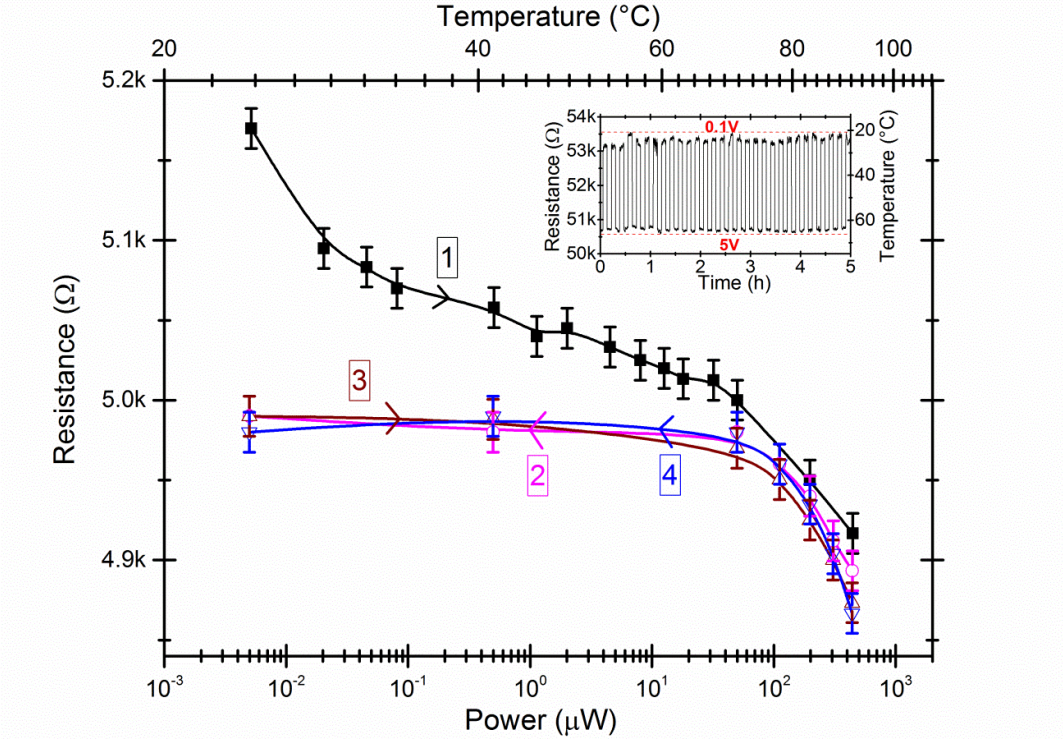

Figure 3. Thermal stabilization sequence. Repetitive behavior after the first cycle was found. Inset: Transient response of a CNF sensor (after stabilization) to square pulses of voltage (0.1V and 5.0V) in SA. Resistance and temperature records show full signal reversibility and stability.

3.3. 2-point calibration procedure

The deposition method leads to sensor devices with different initial resistance values R_o. These values are the macroscopic evidence of different microscopic arrangements and connections in the CNFs mat. The influence of this fact on the calibration and the possibility to obtain a general calibration rule was studied in detail.

Figure 4 presents the calibration curves for four different sensors with R_o values at room temperature ranging from 4.9kΩ to 258kΩ. These results show that the higher the resistance (i.e. less CNF material), the less power was needed to heat the sensors to equivalent temperatures, leading to different threshold in the initial voltage needed to make appreciable the self-heating effect. Unfortunately, we could not find any quantitative and universal relationship between the slope of the temperature vs. voltage calibration and the R_o values, possibly due to the complex combination of heat dissipation and transport mechanisms occurring in the intricate random film. Therefore, specific calibrations should be performed for each and every sensor.

Luckily, all sensors reproduced the linear tendencies described before, opening the door to simplify this calibration step to the determination of just the two extreme points. Figure 4(b) shows that the calibration curve estimated by evaluating the resistance – voltage – temperature connection at room temperature and at a high temperature point is enough to accurately predict intermediate set-points, selected in a fully random sequence ($\sigma = 4.4$°C in deviation with respect nominal calibration values). Therefore, the 2-point calibration is proven to be a fast, reliable and easy method to calibrate the sensors without losing any significant information; being straightforward to imagine how this methodology can be implemented in large scale fabrication processes.

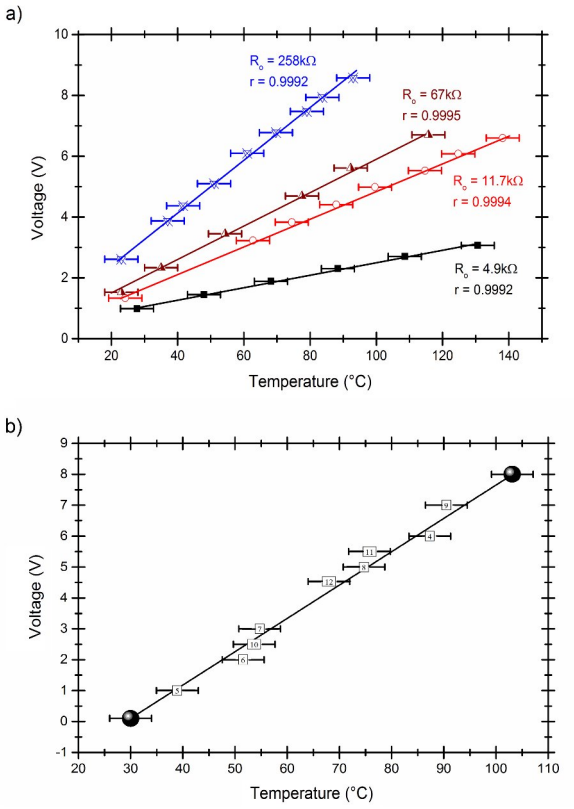

Figure 4. (a) Calibrations of four CNFs sensors presenting different resistance values at room temperature (R_0). (b) Calibration of a sensor using only two points (solid spheres and solid line), the rest of the points, laying close to the calibration line, were measured afterwards to check the validity of the 2-point calibration. The numbers in the boxes correspond to the measurement sequence.

3.4. Application to gas sensing

3.4.1. Humidity

The utility of the self-heating effect occurring in randomly oriented materials to modulate the response to gases was also studied, comparing the response to humidity (one of the most well described target gases for CNF [51]) obtained with an external heater and with self-heating operation.

First, sensors operated at temperatures ranging from 22°C to 115°C were exposed to one single pulse of 95% of relative humidity (RH) (Figure 5). Results show nearly identical response records in both operations modes, demonstrating that equivalent conditions could be achieved by both means. Then, a second test with pulses of 95%, 50%, 25% and again 50% of RH concentrations was carried out to assess the quantification and repeatability potential of the method (Figure 6 shows an example at 45°C), obtaining sensor signals fully reversible, repeatable and linearly proportional to the humidity content.

The gas sensing mechanism for conductometric carbon-based humidity sensors is considered to be the adsorption of water molecules at defective sites of the active material's surface. Water molecules are known to act as electron donors in p-type semiconductors [52,53], such as CNFs. Accordingly, CNFs' electrical resistance increases in presence of water. As water adsorption on carbon surfaces is highly dependent on the nature of the crystalline structure [54] and the nature

of the complex groups previously attached at the carbon surfaces [55], carbonaceous materials can present the full range of adsorption isotherms [56]. As previously stated, the sensor response was linear with concentration, which can be attributed to the low concentration regime predicted by many adsorption models found in the literature [57,58].

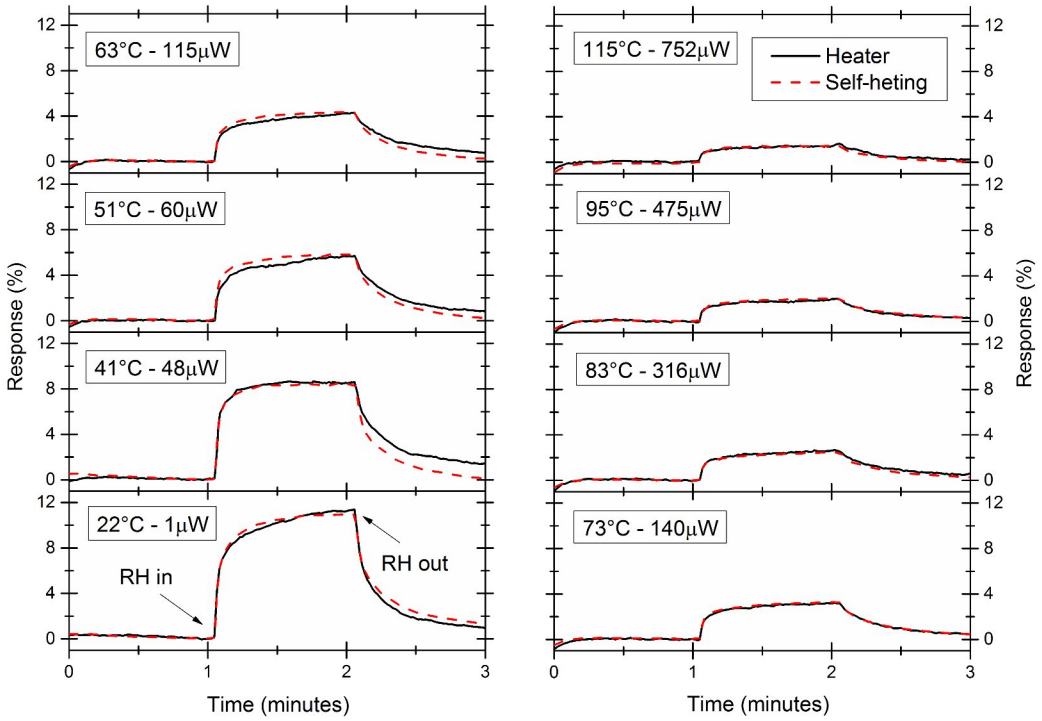

Figure 5. Transient response to one pulse of 95% of RH in SA at different temperatures controlled with an external heater and in self-heating operation. Operation temperature given by heater device and average power consumption in equivalent self-heating operation mode is shown in each panel.

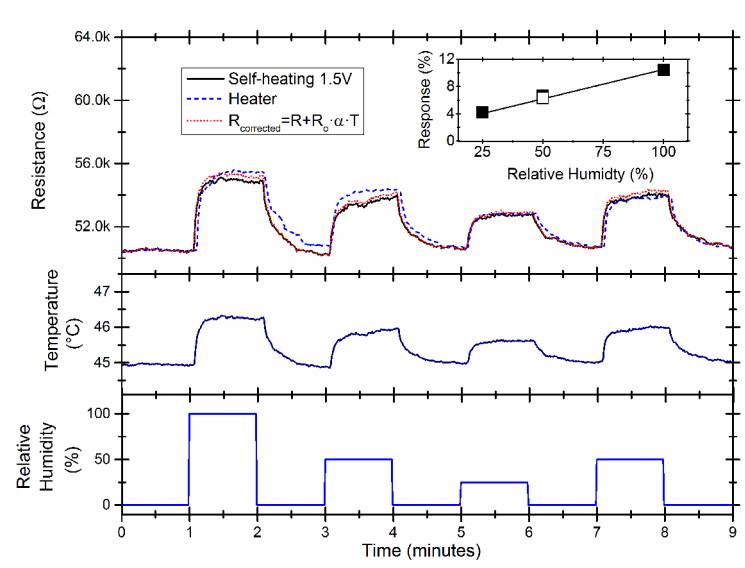

Figure 6. Transient sensor response of a CNF sensor to humidity pulses. Sensor signal obtained by self-heating (1.5V applied to the film) and external heater operation is shown. Transient temperature curve (extracted from power signal) is also represented, the resistance signal correcting the temperature deviation is superposed to sensor signals. Inset: Response dependence with concentration, the white square correspond to the repetition of the pulse at 50% of RH.

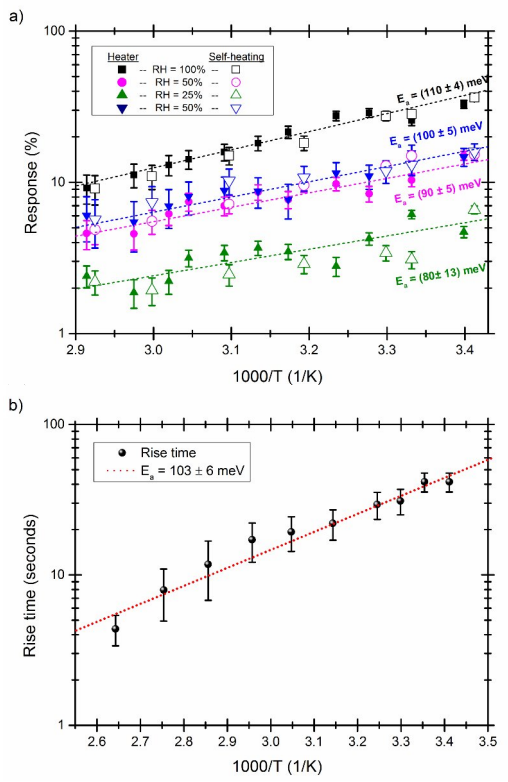

Figure 7. (a) Gas sensor response vs 1000/T obtained for the pulses of 95, 50, 25 and 50% of RH in SA, for temperatures ranging from 22°C to 75°C controlled with an external heater and in self-heating operation. (b) Rise time vs 1000/T shown in an Arrhenius plot.

The sensor response dependence with temperature was also found to be linear in an Arrhenius representation at all concentrations and in both operation modes (see Figure 7). The activation energy values for water adsorption observed in both modes (95 ± 4 meV) were consistent and in accordance with the calculated ones reported elsewhere [59,60].

Response time dependence with temperature is also a direct evidence of a thermally activated process. The Arrhenius representations of the response time lead again to activation energies for water adsorption of 103 ± 6 meV, in agreement with the energies found in the response magnitude (see Figure 7(b)).

Such a coincidence is consistent with the thermal activation of the gas-surface interaction mechanisms expected for water and carbonaceous materials. In a first approximation, the charge transfer, and consequently the sensor response, and consequently can be considered directly proportional to the adsorption isotherm [61]. Moreover, assuming that adsorption follows the Langmuir model [62], the differential transient equation can be written as

$$\frac{d\theta}{dt} = \frac{sP_{tot}C_x}{\sqrt{2\pi m k_B T}} k_o e^{-\frac{E_{ads}}{k_B T}} (1-\theta) - \upsilon e^{-\frac{E_{des}}{k_B T}} \theta \tag{3}$$

where θ is the surface coverage, t is the time, s is the effective surface of a gas molecule, P_{tot} is the total pressure, C_x is the gas concentration, m is the mass of a single molecule, k_b is the Boltzmann constant, T is the temperature, k_o is the sticking probability (also called condensation coefficient), E_{ads} is the activation energy for adsorption, υ is the frequency of oscillation of adsorbed molecules and E_{des} is the activation energy for desorption. The first term of eq. (3) takes into account the adsorption rate and the second term corresponds to the desorption rate. The solution of eq. (3) leads to

$$\theta(t) = \frac{b'C_x}{1+b'C_x}\left(1 - e^{-t/\tau_{resp}}\right) \tag{4}$$

where

$$\tau_{rise} = \frac{k_o s}{\nu\sqrt{2\pi m K_b T}} e^{\left(\frac{E_{des}-E_{abs}}{k_b T}\right)} = b_o e^{\left(\frac{Q}{k_b T}\right)}$$
$$b' = P_{tot} \cdot b_o \cdot e^{\frac{Q}{k_b T}} = b'_o \cdot e^{\frac{Q}{k_b T}} \tag{5}$$

where Q is the adsorption heat ($Q = E_{des} - E_{abs}$) and $b_o = (k_o s)/\left(\nu\sqrt{2\pi M k_b T}\right)$ and $b'_o = P_{tot} \cdot b_o$. From eq. (4) we can clearly see that our definition of response has to be proportional to the term $(b'C_x)/(1+b'C_x)$,

$$\text{Response}(\%) = 100 \cdot \beta \cdot \frac{b'C_x}{1+b'C_x} \tag{6}$$

where β is a the proportionality constant between the response and the coverage θ at $t \to \infty$. As observed in the inset of Figure 6, response was found linear. Thus, the condition needed to consider the response linear to the model is $b'C_x << 1$. Analyzing the order of magnitude of b', using P_{tot} = 1 atm (ambient pressure), k_o = 1 (considering worst case), S = 10Å, $\upsilon = 10^{13}$ s^{-1} [61], T = 300K (near ambient temperature), m = 18 g/mol ~ $3 \cdot 10^{-26}$ kg (H_2O molecular weight), and Q = 0.1 eV (see Figure 7(b)), we obtain a value of $b' \approx 0.5$. As water concentration in air rarely exceeds 4% [63], therefore in a worst case scenario, $b' \cdot C_x \approx 0.02 << 1$. Then, $\text{Response}(\%) \approx 100 \cdot \beta \cdot b'C_x$ and thus, response and response time share the same exponential dependency with Q, explaining the similar activation energy value found in the Arrhenius representation for both magnitudes. In the above analysis the coefficient b_o was considered independent on temperature within the studied range (i.e $\left(1/\sqrt{300K}\right) - \left(1/\sqrt{450K}\right) \approx 8 \cdot 10^{-3} K^{-1/2}$). Summarizing, the Langmuir linear approximation was found to be an appropriate model for water adsorption on CNFs sensors as predicted by the resulting electrical behavior, furthermore the resulting low adsorption heat value extracted from the measured data (~ 0.1eV) agrees with the non-dissociative adsorption used in the model, being these results consistent with other works found in the literature [64–67].

From the power consumption perspective, optimum humidity sensing performances were obtained at 45°C with less than 50μW, to be compared with the 30mW needed for the heater.

All these results demonstrate (1) that the self-heating thermalization can bring a disordered film of nanoparticles to operation conditions fully equivalent to those reached with an external heating system and (2) that this approach is suitable to modulate the response of randomly oriented nanomaterials to gases.

3.4.2. *Other gases*

We have also observed that self-heating is an effective way to modulate the detection of other gases of interest, for which the response of CNF has been reported [51] (Figure 8).

In the case of NH_3, temperature increase rapidly reduces the molecule residence time on the surface, lowering the overall response signal [68]. In the case of NO_2, temperature accelerates the response time and reduces signal drift, but again lowering the response magnitude [68]. All these findings are consistent with the well-known temperature-dependent responses of carbon materials to these target gases.

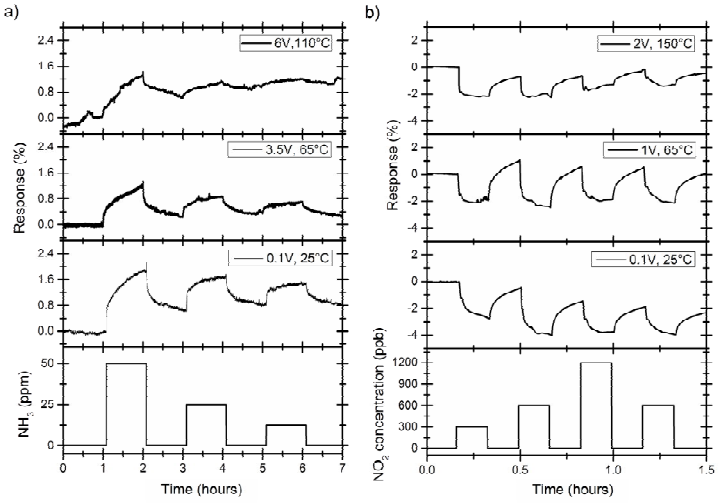

Figure 8. Self-heating modulation for (a) NH_3 and (b) NO_2 gas response.

3.5. **Limitations**

Self-heating in CNFs sensor has been proven to be a useful methodology to operate these simply fabricated devices in low power conditions. However, these findings open new questions deserving further investigation.

A first fundamental issue appears when the same resistance is used to interact with gases and dissipate heat. The resistance change due to gas interaction causes a variation in the electrical power dissipated in the sensor and therefore, in the active's material temperature. To maintain a steady operation point, this gas-induced resistance variation should be small.

In the CNFs sensor, responses are relatively low, assuring a good steady point of operation. For the results shown in Figure 6, a maximum deviation of temperature about 3% was found, meaning a difference of 1.35°C at 45°C. Such a deviation is comparable to the uncertainty in the temperature set-point of standard heating elements [1,40].

The previous point makes us wonder if charge transfer is still the main transduction mechanism, in thermally coupled systems. Charge transfer induced resistance variations may cause temperature differences that could be seen as even larger variations in the overall resistance. To determine the dominant transduction mechanism, we corrected the sensor resistance signal (R) using the temperature dependence described in eq. (1), observing that this correction is small compared to the direct electrical interaction with gases (Figure 6). Therefore, the conductometric nature of CNFs sensors is proven to be the main transduction mechanism.

In any case, the two previous effects strongly depend on the resistance dependence of the active material and would deserve a detailed analysis in future applications to other materials of the here-presented approach.

Finally, carbonaceous materials can degrade, if operated at high temperatures, much easily than other materials typically used for gas sensors (e.g. MOXs [40]). At sufficiently high temperatures, oxygen species contribute to the gasification of carbon, forming CO, CO_2, etc. [69]. This fact limits the temperatures that can be achieved with CNFs in self-heating operation; especially in gas sensing applications, where the presence of additional oxidizing compounds could further accelerate this process.

In order to better understand the effect of gasification in our CNFs sensors, we intentionally tried to burn the CNFs film with self-heating.

Interestingly, we found that the appearance of degradation and eventual destruction was independent on the initial resistance of the film (see supporting information, figure A). This suggests again that the self-heating effect in randomly oriented systems is related to the microscopic arrangement of the nanoparticles. Thus, the films would become useless (i.e. open circuit resistance) when the last conduction paths are destroyed by local heating. In any case, experiments show that such destruction is highly unlikely to occur at moderate operation temperatures.

These results are also an indirect evidence of the local differences of power dissipation due to the dispersion CNFs dimensions, the local heat dissipated by each fiber would be different and also depending on the conduction paths formed during the deposition process. Probably, due to the creation of hot-spot point effect between nanofibers junctions and the heat dissipation variation between nanofibers with different dimensions. These assumptions lead to consider that the gas sensing characteristics of the nanofibers film is modulated locally and differs from one point to another of the nanofibers mat. However, the use of a high amount of randomly deposited CNFs, with its dispersion of diameters and lengths, should compensate the local modification of the film gas sensing properties and consequently, achieving a global self-heating effect through the mat.

Finally, the low specificity is a known issue for carbon based gas sensors [41], self-heating could provide a low power method to improve the differentiation of different target gases through temperature modulation [22].

Therefore, the extension of this principle to other nanomaterials suitable for higher temperature operation (such as MOX or MOX-carbon compounds [70]) and the study of the microscopic temperature variations across randomly oriented films are worth-investigating open questions.

4. Conclusions

We have demonstrated that self-heating effect occurs in films made of randomly oriented nanoparticles (electro-sprayed, drop-casted and paint-brushed films of carbon nanofibers

CNFs), overcoming the complex fabrication requirements of previous attempts and opening the door to the use of this effect in cost effective devices.

Taking advantage of the linear temperature-voltage dependence, a 2-point fast calibration method has also been proposed. This calibration procedure is reliable enough to overcome the lack of reproducibility of low cost fabrication methods.

Self-heating operation made possible reaching temperatures up to 225°C with power consumption in the range of tens of mW, reaching efficiencies comparable to state of the art micro-heaters with a much simpler approach. For certain low-temperature applications (<100°C) typical power consumptions are in the range of tens of μW.

From the applications point of view, the method is suitable to activate the response towards gases, such as humidity, NH_3 or NO_2.

Acknowledgments

The research leading to these results has received funding from the European Research Council under the European Union's Seventh Framework Programme (FP/2007-2013) / ERC Grant Agreement n. 336917.

J.D. Prades acknowledges the support of the Serra Húnter Programme.

A. Cirera acknowledges support from ICREA Academia program.

5. Bibliography

[1] G. Korotcenkov, B.K. Cho, Engineering approaches to improvement of conductometric gas sensor parameters. Part 2: Decrease of dissipated (consumable) power and improvement stability and reliability, Sensors Actuators B Chem. 198 (2014) 316–341.

[2] I. Simon, N. Bârsan, M. Bauer, U. Weimar, Micromachined metal oxide gas sensors: opportunities to improve sensor performance, Sensors Actuators B Chem. 73 (2001) 1–26.

[3] W.-J. Hwang, K.-S. Shin, J.-H. Roh, D.-S. Lee, S.-H. Choa, Development of micro-heaters with optimized temperature compensation design for gas sensors, Sensors. 11 (2011) 2580–2591.

[4] I.-S. Hwang, E.-B. Lee, S.-J. Kim, J.-K. Choi, J.-H. Cha, H.-J. Lee, et al., Gas sensing properties of SnO2 nanowires on micro-heater, Sensors Actuators B Chem. 154 (2011) 295–300.

[5] J.D. Prades, R. Jimenez-Diaz, M. Manzanares, F. Hernandez-Ramirez, A. Cirera, A. Romano-Rodriguez, et al., A model for the response towards oxidizing gases

of photoactivated sensors based on individual SnO2 nanowires., Phys. Chem. Chem. Phys. 11 (2009) 10881–10889.

[6] J.D. Prades, R. Jimenez-Diaz, F. Hernandez-Ramirez, S. Barth, a. Cirera, a. Romano-Rodriguez, et al., Equivalence between thermal and room temperature UV light-modulated responses of gas sensors based on individual SnO2 nanowires, Sensors Actuators B Chem. 140 (2009) 337–341.

[7] L. Deng, X. Ding, D. Zeng, S. Tian, H. Li, C. Xie, Visible-light activate mesoporous WO3 sensors with enhanced formaldehyde-sensing property at room temperature, Sensors Actuators B Chem. 163 (2012) 260–266.

[8] M.W.G. Hoffmann, A.E. Gad, J.D. Prades, F. Hernandez-Ramirez, R. Fiz, H. Shen, et al., Solar diode sensor: Sensing mechanism and applications, Nano Energy. 2 (2013) 514–522.

[9] G. Korotcenkov, Surface Functionalizing of Carbon-Based Gas-Sensing Materials, in: Handb. Gas Sens. Mater., 2014: pp. 359–372.

[10] G. Korotcenkov, Metal Oxide-Based Nanostructures, in: Handb. Gas Sens. Mater., 2014: pp. 47–71.

[11] B. Cho, J. Yoon, M.G. Hahm, D.-H. Kim, A.R. Kim, Y.H. Kahng, et al., Graphene-based gas sensor: metal decoration effect and application to a flexible device, J. Mater. Chem. C. 2 (2014) 5280.

[12] S.C. Colindres, K. Aguir, F. Cervantes Sodi, L.V. Vargas, J.M. Salazar, V.G. Febles, Ozone sensing based on palladium decorated carbon nanotubes, Sensors. 14 (2014) 6806–6818.

[13] G. Neri, S.G. Leonardi, M. Latino, N. Donato, S. Baek, D.E. Conte, et al., Sensing behavior of SnO2/reduced graphene oxide nanocomposites toward NO2, Sensors Actuators B Chem. 179 (2013) 61–68.

[14] A. Esfandiar, A. Irajizad, O. Akhavan, S. Ghasemi, M.R. Gholami, Pd–WO3/reduced graphene oxide hierarchical nanostructures as efficient hydrogen gas sensors, Int. J. Hydrogen Energy. 39 (2014) 8169–8179.

[15] K. Chikkadi, M. Muoth, V. Maiwald, C. Roman, C. Hierold, Ultra-low power operation of self-heated, suspended carbon nanotube gas sensors, Appl. Phys. Lett. 103 (2013) 223109.

[16] N.D. Chinh, N. Van Toan, V. Van Quang, N. Van Duy, N.D. Hoa, N. Van Hieu, Comparative NO2 gas-sensing performance of the self-heated individual, multiple and networked SnO2 nanowire sensors fabricated by a simple process, Sensors Actuators B Chem. 201 (2014) 7–12.

[17] L.F. Zhu, J.C. She, J.Y. Luo, S.Z. Deng, J. Chen, X.W. Ji, et al., Self-heated hydrogen gas sensors based on Pt-coated W18O49 nanowire networks with high

sensitivity, good selectivity and low power consumption, Sensors Actuators B Chem. 153 (2011) 354–360.

[18] J.D. Prades, R. Jimenez-Diaz, F. Hernandez-Ramirez, A. Cirera, A. Romano-Rodriguez, J.R. Morante, Harnessing self-heating in nanowires for energy efficient, fully autonomous and ultra-fast gas sensors, Sensors Actuators B Chem. 144 (2010) 1–5.

[19] E. Strelcov, S. Dmitriev, B. Button, J. Cothren, V. Sysoev, A. Kolmakov, Evidence of the self-heating effect on surface reactivity and gas sensing of metal oxide nanowire chemiresistors, Nanotechnology. 19 (2008) 355502.

[20] J. Zhang, E. Strelcov, A. Kolmakov, Heat dissipation from suspended self-heated nanowires: gas sensor prospective, Nanotechnology. 24 (2013) 444009.

[21] J.D. Prades, R. Jimenez-Diaz, F. Hernandez-Ramirez, S. Barth, A. Cirera, A. Romano-Rodriguez, et al., Ultralow power consumption gas sensors based on self-heated individual nanowires, Appl. Phys. Lett. 93 (2008) 123110.

[22] J.D. Prades, F. Hernández-Ramírez, T. Fischer, M. Hoffmann, R. Müller, N. López, et al., Quantitative analysis of CO-humidity gas mixtures with self-heated nanowires operated in pulsed mode, Appl. Phys. Lett. 97 (2010) 243105.

[23] T.A. Chemical, M.E. Roberts, M.C. Lemieux, Z. Bao, Sorted and Aligned Single-Walled, 3 (2009) 3287–3293.

[24] E. Llobet, Gas sensors using carbon nanomaterials: A review, Sensors Actuators B Chem. 179 (2013) 32–45.

[25] M. Penza, P.J. Martin, J.T.W. Yeow, Gas Sensing Fundamentals, in: Springer Ser. Chem. Sensors Biosens., 2014: pp. 109–174.

[26] G. Korotcenkov, Nanocomposites in Gas Sensors: Promising Approach to Gas Sensor Optimization, in: Handb. Gas Sens. Mater., Springer New York, 2014: pp. 181–184.

[27] Y. Chen, J. Zhang, Chemical Vapor Deposition Growth of Single-Walled Carbon Nanotubes with Controlled Structures for Nanodevice Applications, Acc. Chem. Res. 47 (2014) 2273–2281.

[28] L. Huang, B. Wu, J. Chen, Y. Xue, D. Geng, Y. Guo, et al., Gram-scale synthesis of graphene sheets by a catalytic arc-discharge method, Small. 9 (2013) 1330–1335.

[29] Z. Lin, G.H. Waller, Y. Liu, M. Liu, C. Wong, 3D Nitrogen-doped graphene prepared by pyrolysis of graphene oxide with polypyrrole for electrocatalysis of oxygen reduction reaction, Nano Energy. 2 (2013) 241–248.

[30] C.K. Chua, M. Pumera, Chemical reduction of graphene oxide: a synthetic chemistry viewpoint, Chem. Soc. Rev. 43 (2014) 291–312.

[31] W. Chen, L. Yan, Preparation of graphene by a low-temperature thermal reduction at atmosphere pressure, Nanoscale. 2 (2010) 559–563.

[32] M. Allen, V. Tung, R. Kaner, Honeycomb carbon: a review of graphene, Chem. Rev. (2009) 132–145.

[33] O. Akhavan, K. Bijanzad, A. Mirsepah, Synthesis of graphene from natural and industrial carbonaceous wastes, RSC Adv. 4 (2014) 20441.

[34] K. Paton, E. Varrla, C. Backes, R. Smith, Scalable production of large quantities of defect-free few-layer graphene by shear exfoliation in liquids, Nat. Mater. 13 (2014) 624–630.

[35] G. Lu, L.E. Ocola, J. Chen, Gas detection using low-temperature reduced graphene oxide sheets, Appl. Phys. Lett. 94 (2009) 083111.

[36] T.C. Dinadayalane, J. Leszczynski, Remarkable diversity of carbon–carbon bonds: structures and properties of fullerenes, carbon nanotubes, and graphene, Struct. Chem. 21 (2010) 1155–1169.

[37] M.F.L. De Volder, S.H. Tawfick, R.H. Baughman, a J. Hart, Carbon nanotubes: present and future commercial applications, Science. 339 (2013) 535–539.

[38] A.K. Geim, K.S. Novoselov, The rise of graphene, Nat. Mater. 6 (2007) 183–911.

[39] Y. Zhu, S. Murali, W. Cai, X. Li, J.W. Suk, J.R. Potts, et al., Graphene and graphene oxide: synthesis, properties, and applications, Adv. Mater. 22 (2010) 3906–3924.

[40] G. Korotcenkov, B.K. Cho, Instability of metal oxide-based conductometric gas sensors and approaches to stability improvement (short survey), Sensors Actuators B Chem. 156 (2011) 527–538.

[41] O. Monereo, S. Claramunt, M.M. De Marigorta, M. Boix, R. Leghrib, J.D. Prades, et al., Flexible sensor based on carbon nanofibers with multifunctional sensing features., Talanta. 107 (2013) 239–47.

[42] G. Lu, L.E. Ocola, J. Chen, Reduced graphene oxide for room-temperature gas sensors., Nanotechnology. 20 (2009) 445502.

[43] E. Pop, D. Mann, Q. Wang, K. Goodson, H. Dai, Thermal Conductance of an Individual Single-Wall Carbon Nanotube above Room Temperature, Nano Lett. 6 (2006) 96–100.

[44] Y.A. Kim, T. Hayashi, M. Endo, M.S. Dresselhaus, Carbon Nanofibers, in: Springer Handb. Nanomater., 2013.

[45] S. Claramunt, O. Monereo, M. Boix, R. Leghrib, J.D. Prades, A. Cornet, et al., Flexible gas sensor array with an embedded heater based on metal decorated carbon nanofibres, Sensors Actuators B Chem. 187 (2013) 401–406.

[46] I. Kang, Y.Y. Heung, J.H. Kim, J.W. Lee, R. Gollapudi, S. Subramaniam, et al., Introduction to carbon nanotube and nanofiber smart materials, Compos. Part B Eng. 37 (2006) 382–394.

[47] F.M. Ramos, C. López-gándara, A. Cirera, J.R. Morante, Monolithic Ceramic Technology for Sensing Devices, in: Proc. 2009 Spanish Conf. Electron Devices, 2009: pp. 293–296.

[48] T.R. M. Weisenberger, I. Martín-Gullon, J. Vera-Agullo, H. Varela-Rizo, C. Merino, R. Andrews, D. Qian, The effect of graphitization temperature on the structure of helical-ribbon carbon nanofibers, Carbon. 47 (2009) 2211–2218.

[49] P.G. Collins, Extreme Oxygen Sensitivity of Electronic Properties of Carbon Nanotubes, Science. 287 (2000) 1801–1804.

[50] S.E. Moon, H.-K. Lee, N.-J. Choi, H.T. Kang, J. Lee, S.D. Ahn, et al., Low Power Consumption Micro C2H5OH Gas Sensor based on Micro-heater and Ink jetting Technique, Sensors Actuators B Chem. (2014).

[51] G. Korotcenkov, Handbook of Gas Sensor Materials Volume 2, Handbook of Gas Sensor Materials, 2014.

[52] A. Zahab, L. Spina, P. Poncharal, C. Marliere, Water-vapor effect on the electrical conductivity of a single-walled carbon nanotube mat, Phys. Rev. B. 62 (2000) 0–3.

[53] L. Valentini, C. Cantalini, I. Armentano, J.M. Kenny, L. Lozzi, S. Santucci, Highly sensitive and selective sensors based on carbon nanotubes thin films for molecular detection, Diam. Relat. Mater. 13 (2004) 1301–1305.

[54] C. McCallum, T. Bandosz, S. McGrother, E. Müller, K. Gubbins, A molecular model for adsorption of water on activated carbon: comparison of simulation and experiment, Langmuir. 15 (1999) 533–544.

[55] J. Figueiredo, M. Pereira, M. Freitas, J. Orfao, Modification of the surface chemistry of activated carbons, Carbon. 37 (1999) 1379–1389.

[56] P. Gupta, Water Vapor Adsorption Onto Nanostructured Carbide Derived Carbon (CDC)., University of Illinois at Chicago, 2008.

[57] X. Gao, S. Liu, Y. Zhang, Z. Luo, M. Ni, K. Cen, Adsorption and reduction of NO2 over activated carbon at low temperature, Fuel Process. Technol. 92 (2011) 139–146.

[58] D. Zhang, J. Tong, B. Xia, Humidity-sensing properties of chemically reduced graphene oxide/polymer nanocomposite film sensor based on layer-by-layer nano self-assembly, Sensors Actuators B Chem. 197 (2014) 66–72.

[59] O. Leenaerts, B. Partoens, F. Peeters, Adsorption of H2O, NH3, CO, NO2, and NO on graphene: A first-principles study, Phys. Rev. B. 77 (2008) 125416.

[60] J. Zhao, A. Buldum, J. Han, J. Lu, Gas molecule adsorption in carbon nanotubes and nanotube bundles, Nanotechnology. 13 (2002) 195–200.

[61] M. Gautam, A.H. Jayatissa, Adsorption kinetics of ammonia sensing by graphene films decorated with platinum nanoparticles, J. Appl. Phys. 111 (2012) 094317.

[62] H. Hu, M. Trejo, M. Nicho, S. JM, A. García-Valenzuela, Adsorption kinetics of optochemical NH3 gas sensing with semiconductor polyaniline films, Sensors Actuators B Chem. 82 (2002) 14–23.

[63] A.. Buck, New equations for computing vapor pressure and enhancement factor, J. Appl. Meteorol. 20 (1981) 1527–1532.

[64] G. Korotchenkov, V. Brynzari, S. Dmitriev, Electrical behavior of SnO2 thin films in humid atmosphere, Sensors Actuators B Chem. 54 (1999) 197–201.

[65] J. Ma, A. Michaelides, D. Alfè, L. Schimka, G. Kresse, E. Wang, Adsorption and diffusion of water on graphene from first principles, Phys. Rev. B. 84 (2011) 033402.

[66] F. Yavari, C. Kritzinger, C. Gaire, L. Song, H. Gulapalli, T. Borca-Tasciuc, et al., Tunable bandgap in graphene by the controlled adsorption of water molecules., Small. 6 (2010) 2535–2538.

[67] A. Harding, N. Foley, P. Norman, Diffusion barriers in the kinetics of water vapor adsorption/desorption on activated carbons, Langmuir. 7463 (1998) 3858–3864.

[68] Y. Battie, O. Ducloux, P. Thobois, N. Dorval, J.S. Lauret, B. Attal-Trétout, et al., Gas sensors based on thick films of semi-conducting single walled carbon nanotubes, Carbon. 49 (2011) 3544–3552.

[69] P.A. Campbell, R.E. Mitchell, The impact of the distributions of surface oxides and their migration on characterization of the heterogeneous carbon–oxygen reaction, Combust. Flame. 154 (2008) 47–66.

[70] S. Mao, G. Lu, J. Chen, Nanocarbon-based gas sensors: progress and challenges, J. Mater. Chem. A. 2 (2014) 5573–5579.

Self-heating effects in large arrangements of randomly oriented carbon nanofibers

O. Monereo*, J. D. Prades and A. Cirera
MIND-IN^{2}UB, Department of Electronics, University of Barcelona, C/ Martí i Franquès 1, E-08028 Barcelona, Spain

*Corresponding author e-mail: omonereo@el.ub.edu

Other authors e-mails: J.D. Prades (dprades@el.ub.edu), A.Cirera (acirera@el.ub.edu.)

Author biographies

Oriol Monereo was graduated in Physics at the University of Barcelona in 2010 and in Master in Electronic Engineering in 2011. Now he is Ph.D. student in Department of Electronics of the same university. His current research is focused in gas sensors.

Joan Daniel Prades was born in Barcelona in 1982. He graduated in Physics and Electronic Engineering at the University of Barcelona and obtained his Ph.D. at the same institution in 2009. He has experience in modelling of the electronic and vibrational properties of nanostructured metal oxides and in their experimental validation. He is actively involved in the development of innovative device prototypes based on nanomaterials. He has published more than 40 papers in peer-reviewed journals and contributed to more than 100 international conferences. He has also contributed to five industrial patents.

Albert Cirera is graduated in Physics (1996) and Ph.D. (2000) by the University of Barcelona. He is currently associate professor of the Electronics Department. He has published more than 60 papers in international journals with more than 1000 cited and $h = 19$; as well as more than 100 presentations, 5 book chapters and 5 more patents, he has directed more than 15 industrial and research projects. His current research group deals with computational and applied nanoelectronics, including sensors